1D ANALYTIC MODEL FOR PV AEROMECHANICAL SYSTEMS

RONEN S. LAUTMAN[1], LIRON SHANI[2] & BOAZ NISHRI[1]
[1]CoreFlow Ltd., Israel
[2]Faculty of Engineering, Tel Aviv University, Israel

ABSTRACT
The current work presents a 1D analytic model for a PV aeromechanical system and compares it with a 3D CFD model. The 1D model is based on the analogy between airflow and electric current. A PV aeromechanical system enables accurate positioning of thin, flexible substrates by creating an air cushion between the substrate and an accurate, rigid surface, having bi-directional aeromechanical spring-like behavior. Nozzle can be described as the relation they allow between flow (Q) and pressure drop (Δp): $R \propto \Delta p/Qn$ where n depends on the characteristic behavior and (in this work) is between 1 and 2. The 1D model is computationally much cheaper than the 3D CFD model. Although the 1D model requires one CFD 3D model analysis for quantifying the exact resistance in the air cushion, it allows very fast calculations of performance when varying the other parameters of air gap, pressure/vacuum supply, and flowrate. The difference between 1D analytic model and full CFD analysis, in terms of air gap stiffness results was approximately 3%.
Keywords: CFD, air cushion, aeromechanical spring, analytic model.

1 INTRODUCTION

This paper presents a relatively simple 1D model for analysis of an accepted technique for accurate positioning and maintaining thin flexible substrate positioning over a surface where non-contact with the substrate is beneficial. PV aeromechanical systems include a rigid surface with periodic distribution of openings which supply either pressure or vacuum, as well as appropriate connections to pressure and vacuum supplies (typically air or N_2 gas). A thin substrate covering the rigid surface will experience the pressure as a force directed away from the surface, and the vacuum as a force directed toward the surface. The distance between the substrate and rigid surface is called an air gap or air cushion. The pressure field in the air gap is determined by the pressure/vacuum supplies, the air gap height, and the nozzles which are located between the pressure/vacuum supplies and the air gap. These nozzles require a significant pressure drop to allow flow through them, thus allowing the net force on the substrate to be zero at the non-zero equilibrium air gap. At an air gap smaller than equilibrium the net force acting on the substrate is directed away from the surface; at an air gap larger than equilibrium the net force acting on the substrate is directed toward the surface. The changing air gap height requires a change in flowrate. The changing flowrate through each nozzle requires a change in the pressure drop across each nozzle. Thus, the nozzles allow a uniform, constant pressure supply to result in a differing pressure field on a substrate, which will be a net force on the substrate in the direction toward equilibrium. This relationship between air gap height and force can be quantified into a bi-directional aeromechanical spring-like stiffness [1].

Typically, traditional 3D CFD models are used to predict behavior of the airflow through the air gap. The 3D model can be detailed enough to capture the airflow yet would require the solution to the Navier–Stokes equations in every cell of the model. A 1D model, by contrast, would substitute significant portions of a 3D model with a single equation which takes advantage of an analogy between Ohm's Law and airflow through a resistor. Post-

WIT Transactions on Engineering Sciences, Vol 120, © 2018 WIT Press
www.witpress.com, ISSN 1743-3533 (on-line)
doi:10.2495/AFM180221

processing analysis allows for prediction of net forces acting on the substrate in the event of a non-equilibrium air gap.

Air cushion stiffness is the most significant performance parameter of PV aeromechanical systems. It determines both the static performance, and dynamic performance. To take two examples from the field of Flat-Panel Display (FPD), static performance is required in inspection applications which use "step-and-scan" methodologies, and dynamic performance is required in coating applications where a substrate moves over a PV platform while coating material is being deposited with a tight tolerance.

2 3D AND 1D MODELS

The 3D model was calculated using finite-volume based CFD software Fluent. The analysis domain is presented in Fig. 1. The distance d between pressure and vacuum openings is selected to be small enough that substrate deformation due to local pressure extrema is very small. As a result, the basic cell pressure-vacuum field can be represented by single net force: the pressure-vacuum field integration over the basic cell.

The CFD analysis domain encloses one pressure opening and one vacuum opening. The boundaries of the analysis domain as the rigid surface and the thin substrate surface (impermeable walls). The analysis domain approximates an infinitely large rigid surface, and so there is an explicit assumption made that the flow between the pressure and vacuum openings are periodic in the two directions normal to the air gap height. The periodic boundaries are shown in thick black lines in Fig. 1(b).

The inlet to the analysis domain is simulating a reservoir at constant pressure, and the outlet is simulating a reservoir at constant vacuum. Inside of the opening of the pressure nozzle is a volume of calculation cells which are governed by the characteristic behavior of the pressure nozzle, $R_p = \Delta P/Q^{np}$. Inside the opening of the vacuum nozzle is a volume of calculation cells which are governed by the characteristic behavior of the vacuum nozzle, $R_v = \Delta P/Q^{nv}$.

The numerical mesh was a structured grid of hexahedrons. The mesh was defined very finely in the vicinity of the pressure and vacuum openings, and more coarsely near the periodic boundaries where the flow was expected to change slower. There were 714,812 elements in the model whose solution was found to be grid independent [3].

Fig. 2 shows (a) velocity field and (b) pressure field distribution resulting from the CFD analysis. Both the pressure and velocity fields show almost 1D axisymmetric distribution near the pressure/vacuum openings where the velocity is high and most of the flow resistance is induced in the air gap. It was therefore hypothesized that it is possible to model the flow through the air gap by single 1D flow resistor as a function of air gap height, $R_{ac}(\varepsilon)$. Once $R_{ac}(\varepsilon)$ is defined, it is possible the model the entire PV flow circuit from pressure reservoir to vacuum reservoir by well-known analogy between flow and electric circuits, as in [5]. The 1D model is shown schematically in Fig. 3.

The PV system is modelled in Fig. 3 by voltage divider electric circuits with 3 nonlinear resistors: R_{pnoz} represents the pressure nozzle, R_{vnoz} represents the vacuum nozzle, and R_{ac} represents the flow in the air cushion between flexible substrate and the base rigid surface. The flow is driven by constant pressure gradient between pressure and vacuum supply reservoirs P_{sup} and V_{sup}, respectively. The flow is in steady state, all gas passages have infinite mechanical stiffness and therefore the analogous circuit includes only resistance.

2.1 Nozzles resistance R_p and R_v

Nozzles as flow resistance is characterized by Darcy–Forchheimer relation in eqn (1) that was originally formulated for flows in permeable porous media in [2].

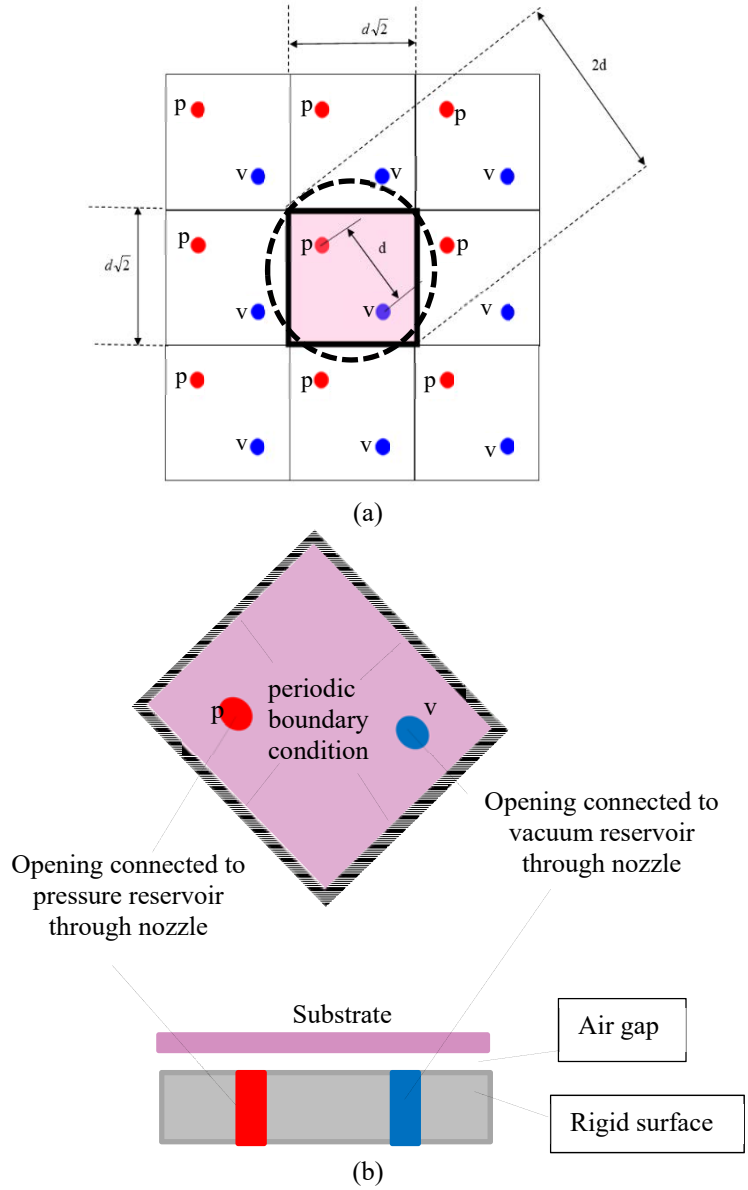

Figure 1: (a) Outline of distribution of pressure and vacuum openings in a rigid surface. The distance between neighboring openings is d. The repeating nature of the distribution allows analysis of only a small cell with periodic boundary conditions; (b) Top and side views of the basic structure of the CFD analysis domain. The inlet is the opening for a pressure nozzle, which is simulated as a reservoir at constant pressure. The outlet is the opening for a vacuum nozzle, which is simulated as a reservoir at constant vacuum. The air gap is of constant height. The substrate and rigid surface are modelled as non-slip walls. The boundaries in the four other sides are modelled as periodic.

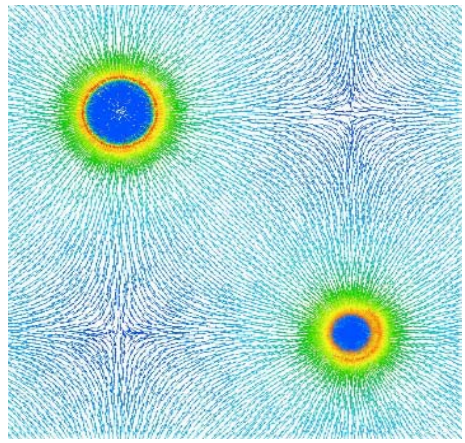

(a)

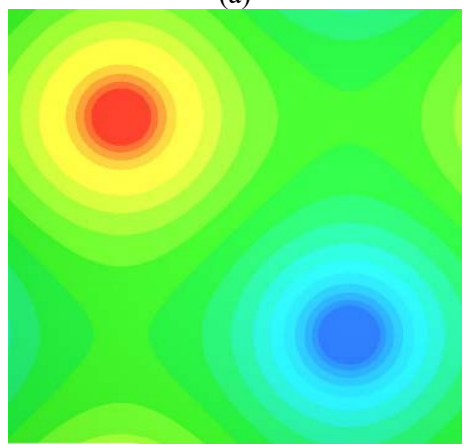

(b)

Figure 2: (a) Velocity field distribution of the 3D CFD model; (b) Pressure field distribution of the same.

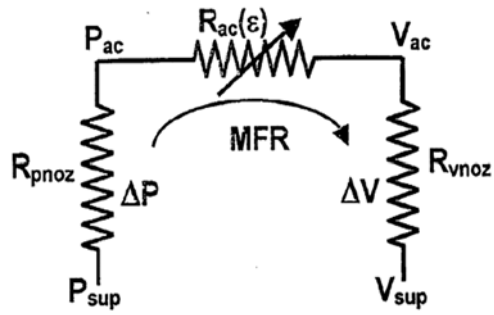

Figure 3: 1D model of air gap from pressure supply reservoir (P_{sup}), through the pressure side nozzle (R_{pnoz}), through the air cushion ($R_{ac}(\varepsilon)$), through the vacuum side nozzle (R_{vnoz}), to the vacuum supply reservoir (V_{sup}).

$$-\frac{\Delta P}{L} = \alpha\mu V + \beta\rho V^2, \tag{1}$$

where $\Delta P/L$ is pressure drop per length, μ is gas viscosity, V is average gas velocity, ρ is gas density, α and β are two constants: α related to the viscous term and β to the inertial term. To describe PV nozzles behavior, Darcy–Forchheimer may simplified to a relation between flow rate (Q) and pressure drop (ΔP) (eqn (2)). k is about constant for small ΔP. The model for the pressure nozzle R_{pnoz} is presented in eqn (4) and the model for the vacuum nozzle R_{vnoz} is presented in eqn (5)

$$\Delta P = k * Q^n, \tag{2}$$

$$R = \frac{\Delta P}{Q} = k * Q^{n-1}, \tag{3}$$

$$R_{pnoz} = k_p * Q^{np-1}, \tag{4}$$

$$R_{vnoz} = k_v * Q^{nv-1}. \tag{5}$$

2.2 Air cushion resistance (R_{ac})

Typical maximum Reynolds number (Re) for PV air cushion is approximately 50 and the flow is laminar. There are several references that present analytic solution for laminar axisymmetric flow between two parallel plates. For example, eqn (6) from [4]:

$$p(r) = k_i \frac{\rho Q^2}{\varepsilon^2}\left[\frac{1}{R^2} - \frac{1}{r_2^2}\right] + k_{vis}\frac{Q\mu}{\varepsilon^3} ln\left(\frac{R}{r}\right) + P(R),$$
$$k_i = \frac{27}{140\pi^2} \text{ and } k_{vis} = \frac{6}{\pi}. \tag{6}$$

Eqn (6) has an inertial term including k_i and a viscous term including k_{vis}. In typical PV systems the inertial term is two orders of magnitude smaller than the viscous term, and so can be neglected in most cases. Eqn (6) thus reduces to eqn (7), and the resistance of the air cushion defined as in eqn (8)

$$\Delta P_{ac} = 2\frac{k_{vis}*Q*\mu}{\varepsilon^3}\ln\left(\frac{d}{2r}\right), \tag{7}$$

$$R_{ac} = \frac{\Delta P_{ac}}{Q} = \frac{k_{ac}}{\varepsilon^3}, \tag{8}$$

where R_{ac} is the air cushion resistor, r is the opening radius, d is the distance between two adjacent opening, and k_{ac} is a constant.

3 1D MODEL ANALYSIS PROCEDURE

The 1D model shown in Fig. 3 can be described using the relationships between flowrate, pressure drop, and resistance to flow in eqns (4), (5), and (8). The model is brought in eqn (9).

$$Q = \frac{P_{sup} + \left|V_{sup}\right|}{\frac{K_{ac}}{\varepsilon^3} + K_p \cdot Q^{np-1} + K_V \cdot Q^{nv-1}}. \tag{9}$$

In this work, the goal-seek analysis built into Microsoft Excel was used to solve the non-linear eqn (9) to find the relation $Q = f(\varepsilon)$, though any iterative procedure may be used to reproduce these results. The forces may be calculated by integration over ΔP_{ac} (eqn (7)). In

this work a simplifying assumption was made that the net force over the glass F is proportional to P_{ac}-$|V_{ac}|$, as in eqn (10)

$$F=K*(P_{ac}-|V_{ac}|), \tag{10}$$

$$P_{ac} = P_{sup} - K_p \cdot Q(\varepsilon)^{np}, \tag{11}$$

$$|V_{ac}| = |V_{sup}| - K_v \cdot Q(\varepsilon)^{nv}, \tag{12}$$

$$Stiffness_{1-2} = K\frac{\left(P_{ac}-|V_{ac}|\right)_{\varepsilon 2}-\left(P_{ac}-|V_{ac}|\right)_{\varepsilon 1}}{\varepsilon_2-\varepsilon_1}. \tag{13}$$

In order to solve eqns (9)–(13), five constants need to be defined: K_v, K_p, K_{ac}, n_p and n_v. If given an arbitrary value, K in eqn (13) can be used for comparative purposes only. For real physical value, K for stiffness per cell area (in units fore/area per length) is ~0.5. K_{ac} for pure axisymmetric flow is defined by eqns (6), (7), and (8), and is brought in another form in eqn (14)

$$K_{ac} = 2k_{vis} * \mu * \ln\left(\frac{d}{2r}\right), \tag{14}$$

k_{vis} is the constant viscose term in eqns (6) and (7). Fig. 4 presents the inertia force portion calculated from eqn (6) in the flowrate range of 0.1 L/min to 1.0 L/min, which covers most typical applications. It is evident that the assumption for constant K_{vis} may lead to ~10% at high flow and gap height. This error can be significantly reduced by performing single 3D CFD analysis to calculate the specific configuration flow rate Q' at given $\Delta P'_{ac}$ and gap height ε', and defined K_{ac} for specific configuration, using eqn (8), as show in eqn (15)

$$K_{ac} = \frac{\varepsilon'^3 \Delta P'_{ac}}{Q'}. \tag{15}$$

Once the constant K_{ac} is defined, there are several ways to use eqn (9). Constrains or requirements needs to be defined in order to get a unique solution. For example, in most applications the nominal (equilibrium) flow rate Q, pressure supply P_{sup}, vacuum supply V_{sup} and gap height ε are common requirements. Given these four constrains and assuming that the nozzles characteristic exponent n_p and n_v are the free investigation parameters, the following sequence can be applied:

- Given investigated nozzles characteristic exponents n_p and n_v.
- $\Delta P_{ac}=K_{ac}*Q/\varepsilon^3$ (using eqn (8)).
- $P_{ac}=|V_{ac}|= 0.5*\Delta P_{ac}$ (the substrate is at equilibrium).
- Pressure drop across the pressure nozzle $\Delta P_p = P_{sup}-P_{ac.}$
- $K_p= \Delta P_p /Q^{np}$ (from eqn (2)).
- Vacuum drop across the vacuum nozzle $\Delta V_v = V_{sup}-V_{ac.}$
- $K_v= \Delta V_v /Q^{nv}$ (from eqn (2)).

Eqns (9)–(13) can then solve for different gap height to find the PV response to substrate deviation from its equilibrium state.

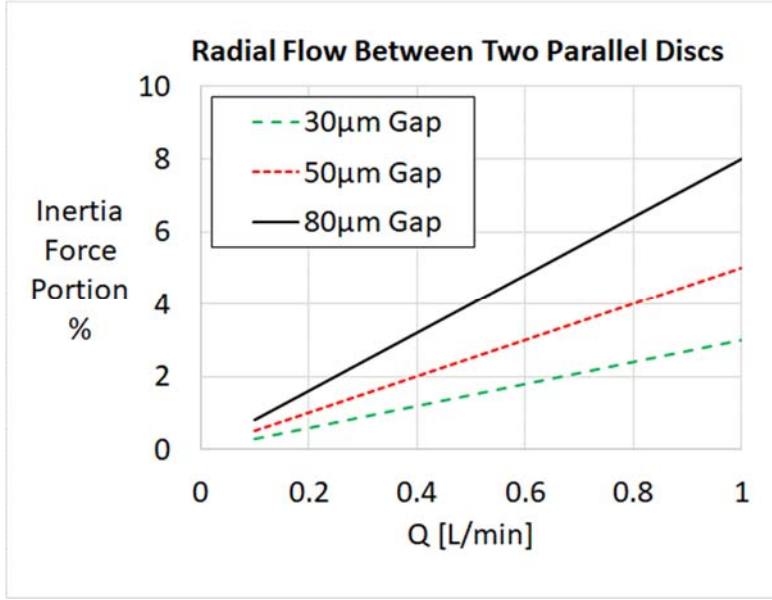

Figure 4: Inertial portion of the force from eqn (6).

4 RESULTS

Fig. 5 presents an example comparison between results from the 1D model and 3D CFD model. The 1D model force F in Fig. 5(b) was taken as $0.5*A*(P_{ac}–V_{ac})$, where A is the wetted area of the substrate in the analysis domain. The 3D CFD model force is the integration of the pressure over the wetted area of the substrate in the analysis domain. Normalized stiffness in Fig. 5(c) is the derivative dF/dε. The equilibrium air gap is 50 µm, where the net force is 0 N, and the stiffness at this air gap is normalized to unity.

Table 1 is a summary of 7 different PV design cases, comparing between the stiffness at equilibrium air gap found using the 1D model and the 3D CFD model. All 1D models use the same K_{ac}, defined by eqn (15), based on single CFD analysis. The free parameter was the nozzles characteristic exponent *np* and *nv* (eqn (3)). The normalizing value for all cases was the *np=nv=2* case (Fig. 5). The error was calculated according to eqn (16)

$$Error = \frac{|Stiffness(3D) - Stiffness\ (1D)|}{Stiffness(3D)}. \tag{16}$$

5 DISCUSSION AND SUMMARY

The current work presents 1D analytic model for aeromechanical analysis and compares it with a 3D CFD model. The 1D model is useful for low-flow regions, allowing to make two assumptions: (1) the air cushion flow is axisymmetric, and (2) the air cushion inertia force is very small in comparison with the viscous forces and thus may be neglected. The results show that the different between the 1D analytic model and full CFD analysis "fluid-dynamic stiffness" results was approximately 3%. The 1D model is computationally much cheaper than the 3D CFD model. Although the 1D model requires one CFD 3D model analysis for quantifying the exact resistance in the air cushion, it allows very fast calculations of performance when varying the other parameters of air gap, pressure/vacuum supply, and flowrate.

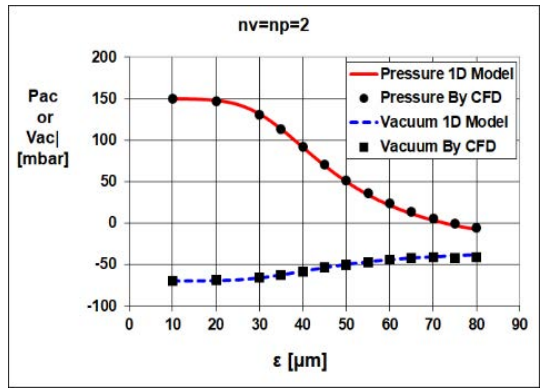

(a)

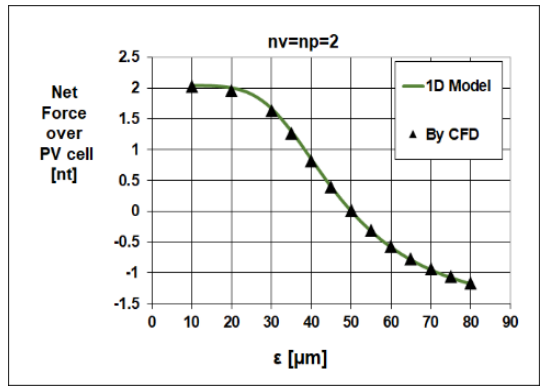

(b)

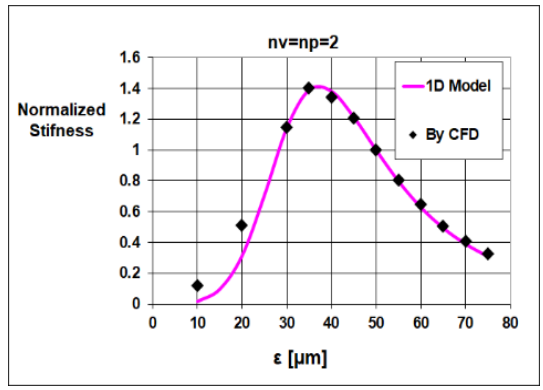

(c)

Figure 5: Typical comparison between results from 3D CFD and 1D models. (a) Values for P_{ac} and V_{ac} at as the substrate deviates from equilibrium air gap height; (b) Net force acting on the substrate as the substrate deviates from equilibrium air gap height; (c) The stiffness of the air gap, calculated as a one-sided numerical derivative of the net force.

Table 1: Comparison between 1D and 3D models.

Nozzle characteristic *n*		Normalized stiffness =(%)		
Pressure, *np*	Vacuum, *nv*	1D model	3D CFD model	Error (%)
2	2	103	100	2.8
1	1	79	80	1.75
1	2	51	52	2.25
2	1	119	121	1.2
1.3	1.3	87	86	1.8
1.7	1.7	95	96	1.2
1.7	1.3	107	109	1.7

REFERENCES

[1] Yassour, Y., Richman, H. & Levin, D., High-performance non-contact support platforms. US Patent 7530778B2, 2009.
[2] Andrade, J.S. et al., Inertial effect on fluid flow through disordered porous media. *Physical Review Letters*, **82**(26), pp. 5249–5252, 1999.
[3] Armengol, J. et al., Bernoulli correction to viscous losses; radial flow between two parallel discs. *American Journal of Physics*, **76**, pp. 730–737, 2008.
[4] Shani, L., Nozzles characteristic effect on PV air cushion performance study. MSc thesis, Faculty of Engineering, Tel Aviv University, 2015.
[5] Oh, K.W. et al., Design of pressure-driven microfluidic network using electric circuit analogy. *The Royal Society of Chemistry Journal*, **12**, pp. 515–545, 2012.